Energy Proceedings
Vol 26, 2022
ISSN 2004-2965

Ni-Co oxide anchored carbon dots for high-performance asymmetric supercapacitor

Prerna Sinha[1] and Kamal K. Kar[1,2*]

[1]Advanced Nanoengineering Materials Laboratory, Materials Science Programme, Indian Institute of Technology Kanpur, Kanpur-208016, India.

[2]Advanced Nanoengineering Materials Laboratory, Department of Mechanical Engineering, Indian Institute of Technology Kanpur, Kanpur-208016, India

ABSTRACT

Nickel–cobalt oxide and carbon dots (Ni-Co oxide@C-dots) nanocomposite were prepared by hydrothermal synthesis followed by the pyrolysis technique. The nanocomposite exhibited a flower-like morphology with porous and interconnected monoliths. The nano-dimension carbon dot pockets throughout the composites provide an efficient resistance-free electron transfer pathway. Also, flower-petals type morphology at the surface attracts and enhances electrolyte-electrode interaction. Hence, Ni-Co oxide@C-dots act as a potential anode for a hybrid supercapacitor. As a negative electrode, a high-performance human hair-derived activated carbon is used. In asymmetric assembly, the device delivers a specific capacitance of 295 F g^{-1} at 1 A g^{-1}. The device also exhibits an excellent energy density of 92 Wh kg^{-1} at a power density of 1000 W kg^{-1}. The study suggests the synthesis and assembly of a high-performance energy storage device.

Keywords: Energy storage system, supercapacitor, charge storage, renewable carbon, waste human hair, Ni-Co oxide@C-dots

NOMENCLATURE

Abbreviations	
SEM	Scanning electron microscopy
XPS	X-ray photoelectron spectroscopy
Symbols	
mV s^{-1}	Milli-volt per second
F g^{-1}	Farad per gram
A g^{-1}	Ampere per gram
Wh kg^{-1}	Watt-hour per Kilogram
W kg^{-1}	Watt per kilogram

1. INTRODUCTION

Most of the energy demands are fulfilled by non-renewable energy sources, which are depleting at a fast rate. There is a need to generate renewable resources and develop energy storage systems to store the energy for the desired application. Presently, various energy storage systems are available with limitations. The batteries are widely used as energy storage devices, but their applications are restrained. The batteries have high energy density but fail to deliver high power in a short period. Supercapacitors are another energy storage system that has gained significant attention due to their simple charge storage process, non-toxic components, and superior device stability. However, the considerable limitation of commercialization is its poor energy density.

Depending on the charge storage mechanism, supercapacitors can be classified as electric double-layer capacitors (EDLC) and pseudocapacitors. However, both processes have their inherent advantages and limitations. EDLC utilizes carbon material that undergoes an electrostatic type charge-storage process. Here, a bilayer formation occurs at the electrode-electrolyte interface via the adsorption of electrolytic ions. A physical process is involved during charge storage, so EDLCs show excellent device stability. In pseudocapacitance, metal oxide and conducting polymers are used that stores charge by a Faradaic mechanism. Here, electron transfer occurs by changing the oxidation state of electrodes via a reversible redox reaction [1]. However, both classes of materials suffer from inherent limitations. Since surface activity is involved in the EDLC, it delivers poor capacitance, whereas metal oxide shows a high capacitance value but degrades due to poor conductivity and electrode stability [2]. A hybrid electrode can be used to combine the two traditional materials that can act as an ideal electrode for a supercapacitor. In a hybrid electrode, the presence of metal oxide provides high capacitance and carbon materials, undergoes capacitive charge storage, enhances conductivity, and provides mechanical support

to the electrode material. Also, in addition to improving the electrode material, an asymmetric hybrid device assembly can improve the device performance by widening the device working potential, thereby improving the energy density.

In an asymmetric assembly, carbon-based materials are generally used as a negative electrode, and metal oxide composites as a positive electrode. Both electrode working potential is utilized in this configuration, thereby improving the overall cell voltage.

Based on the above viewpoints, a high-performance asymmetric device is designed using simple pyrolysis and hydrothermal techniques. A hybrid nanocomposite of Ni-Co oxide and carbon dots is synthesized using hydrothermal synthesis as a positive electrode. The composite exhibit an interconnected flower-like porous morphology. The presence of porosity provides a high surface area improving the accessibility of the electrolyte ions. Also, the interconnected flower-like morphology improves the electrode-electrolyte interaction and provides resistance-free transportation of electrons to the external circuit. Also, the presence of carbon dots pockets throughout the Ni-Co oxide matrix enhances the conductivity of the nanocomposite. On the other hand, activated carbon is used as a negative electrode prepared from waste biomass-human hair. The carbonization followed by KOH activation of the human hair yields a three-dimensional highly porous activated carbon (AC). AC undergoes an EDLC-type charge-storage process. However, incorporating a small fraction of nitrogen, oxygen, and sulfur functionalities from the inorganic species in human hair enhances the performance by providing additional pseudocapacitance to the device. The present study suggests a cost-effective, environment-friendly hybrid electrode for a high-performance supercapacitor.

2. MATERIALS AND METHODS

Materials: Glucose (Glucon D, Zydus Wellness), nickel nitrate hexahydrate ($Ni(NO_3)_2.\ 6H_2O$, Alfa Aesar), cobalt nitrate hexahydrate ($Co(NO_3)_{2.6}\ H_2O$), Alfa Aesar), Urea (CH_4N_2O, local market), citric acid ($C_6H_8O_7$, lemon juice), Potassium hydroxide (KOH, Alfa Aesar), Deionized water was employed throughout the investigation for the treatment processes.

Methods:

Synthesis of a positive electrode, Ni-Co oxide@C-dots: Nickle nitrate and cobalt nitrate were mixed in a 1:2 ratio in (15 ml DI water+15 ml ethanol). C-dots precursor, glucose was mixed in the above solution. The ratio of Ni-Co precursor and C-dots precursor was 1:1. Urea was added to the solution, which acted as a catalyst to promote the reaction. The solution was evenly mixed and transferred in the Teflon-lined autoclave. The autoclave was kept in the oven at 180 ^{o}C for 10 hr. The obtained solution was centrifuged to eliminate the solute from the solvent. The slurry was kept in the oven to eliminate water content. After that, the dried powder was pyrolyzed in N_2 atmosphere at 500 ^{o}C for 1 hr.

Synthesis of a negative electrode activated carbon: Waste human hair was collected from the barbershop at IIT Kanpur. The hair was washed with tap water to remove dirt, followed by DI water and ethanol. The hair was dried in the oven at 60 ^{o}C. The dried hair was cut into small fragments ~2 cm. The hair fibers were carbonized in a tubular furnace at 900 ^{o}C for 1 hr, with an isothermal hold at 220 ^{o}C for 1.5 hr. The carbonized char was finely grounded and mixed with KOH in 1:4 ratio for activation at 900 ^{o}C for 1 hr. The obtained powder was washed with 1 M HCl followed by DI water until neutral pH was achieved.

3. EQUATION USED

a) Energy density is the amount of energy stored per kg in the device.

The accurate energy density of the device is expressed as,

$$E = \frac{\text{area under the discharge curve x current applied}}{\text{mass of both the electrodes}}$$

b) Power density is the rate at which the stored energy is transferred from the device.

The accurate power density of the device is expressed as,

$$P = \frac{E}{\text{area under the discharge curve}}$$

c) Capacitance: It is the ability of a device to store charge with respect to potential.

The capacitance of the device is expressed as,

$$C = \frac{2 \times E}{\Delta V^2}$$

d) Coulombic efficiency: It is the discharge capacity ratio to the charge capacity. It quantifies the losses occurring from the charging to discharging state of the device.
The Coulombic efficiency is expressed as,

$$\eta\ (\%) = \frac{\text{Area under the discharge curve}}{\text{Area under the charge curve}} \times 100$$

4. RESULTS AND DISCUSSION

4.1 Material characterization studies of the as-synthesized electrodes

The activated carbon prepared by carbonization and KOH activation suggests successfully synthesizing highly porous carbon from a waste biomass-human hair. Fig. 1a shows the SEM micrograph of AC. The generation of porosity can be observed. The presence of a pore increases the surface area, thereby improving the electrode capacitance. Also, the interconnected carbon monolith morphology provides resistance-free ion transportation. The as-synthesized activated carbon is used as a negative electrode in asymmetric device assembly.

On the other hand, the nanocomposite Ni-Co oxide@C-dots synthesized via hydrothermal procedure followed by low-temperature pyrolysis depicts the homogeneous flower-like morphology, as presented in Fig. 1b. Homogeneous morphology suggests a single phase composition of nickel cobalt oxide and C-dots species. The existence of C-dots throughout the matrix provides a resistance-free electron transport pathway. Also, it provides mechanical support to the nanocomposites by binding Ni-Co oxide among each other. The flower petals-like morphology emerging from the surface provides a large surface area for the electrode-electrolyte interaction. The nanocomposite contains carbon, nickel, cobalt, and oxygen elements. The elemental composition of the nanocomposite has been studied via XPS analysis. Generally, the spectra obtained from XPS contain overlapped peaks. The deconvolution of the spectra into a different peak is required to obtain the binding states of the elements. Here, XPS peak 4.1 software is used to deconvolute the elemental spectra. The deconvoluted spectra of the respective elements are presented in Fig. 1c-f. The C 1s spectra suggest the binding carbon element with oxygen in sp^3 hybridization. Also, the presence of sp^2 hybridized carbon along with –C-O-C- and –C=O functionalities, as shown in Fig. 1c [3]. The O 1s spectra in Fig. 1d depict the presence of oxygen atoms as metal oxides and carbonyl and quinone groups. Further, Fig. 1e and f show the deconvoluted spectra of Ni 2p and Co 2p. The elements show the peak for +2 and +3 oxidation states with their corresponding satellite peaks [4]. Variable oxidation states illustrate that the Ni and Co species can easily undergo reversible redox reactions to provide pseudocapacitance.

4.2 Electrochemical studies of Ni-Co oxide@C-dots //AC

*T*he electrochemical studies of the asymmetric device were performed in a homemade 2-electrode assembly. The electrode powders were placed in the stainless steel sheet, which acts as a current collector. A filter paper dipped in 6 M KOH electrolyte was placed above the stainless steel-coated electrode. After that, the current collector-coated electrode was placed above the filter paper. The whole assembly was placed between the acrylic sheets and secured with screws.

The electrochemical studies were performed in Metrohm Autolab potentiostat. The electrochemical measurement cyclic voltammetry (CV) and galvanostatic charge-discharge (GCD) were performed. CV test in the device is carried out by linearly changing the electric potential from positive to negative electrode. The obtained current value depends upon the speed of the potential change in mV s^{-1}, called scan rate. In a supercapacitor, the area under the CV loop depicts the charge stored by the device. GCD, on the hand, shows the device performance through the repetitive charge-discharge process. Here, the time taken for charging and discharging is recorded by applying constant current density at a specific voltage range. GCD is a versatile and accurate testing method for analyzing device performance. The capacitance, Coulombic efficiency, iR drop, energy, and power density are calculated using GCD data [5].

Fig. 2a displays the CV curve at a different potential window at a sweep rate of 50 mV s^{-1}. The CV curve suggests that after 1.6 V, the anodic peak appears, indicating the decomposition of water in the electrolyte. Hence, the device delivers a stable potential window of 0-1.6 V. The advantage of asymmetric configuration can

be observed where the device illustrates a stable potential window of 1.6 V in an aqueous electrolyte. The electrolysis of water starts at 1.23 V, but with asymmetric, the decomposition potential shifts beyond 1.6 V [6]. Fig. 2b depicts the CV curve at different scan rates. The curve indicates capacitive charge storage till 0.6 V; a sharp increase in the current is observed, indicating the Faradaic type charge-storage process. Here, Ni and Co change their oxidation states, generating electrons, and the presence of carbon species throughout the matrix efficiently transports it to the external circuit. It is worth noting that no prominent redox peak is observed due to nano-dimensional flower-like morphology. It enables the participation of a large amount of surface for electrolyte ion adsorption and reversible reactions. Hence, the advantage of the hybrid electrode can be clearly seen where two different electrode materials provide a synergistic charge storage process that increases the performance of the device.

The traditional electrode undergoes either ELDC or Faradaic type charge-storage process. These include carbon materials that store charge by bilayer formation at the electrode-electrolyte interfaces. Here, the physisorption of ions takes place at the electrode surface. Since no chemical processes are involved, carbon material shows exceptional device stability upon the charge-discharge process. However, it delivers poor capacitance as the charge storage process is limited to the available surface. Another type of charge storage is via the Faradaic mechanism, where pseudocapacitance is generated. Metal oxide/hydroxides generally undergo a reversible redox reaction to store charge. Here high capacitance value is achieved as electron transfer takes place. However, apart from RuO2, an expensive electrode, othe metal oxides suffer from poor conductivity, decreasing the rate capability and stability of the electrode. Using composite electrodes is an effective strategy to exploit the advantage of traditional electrodes. Here, the metal oxide will undergo a reversible redox reaction to generate a large amount of electrons, and the presence of carbon will help these electrons get transferred to the current collector. Also, carbon electrodes will provide mechanical support, improving the device stability.

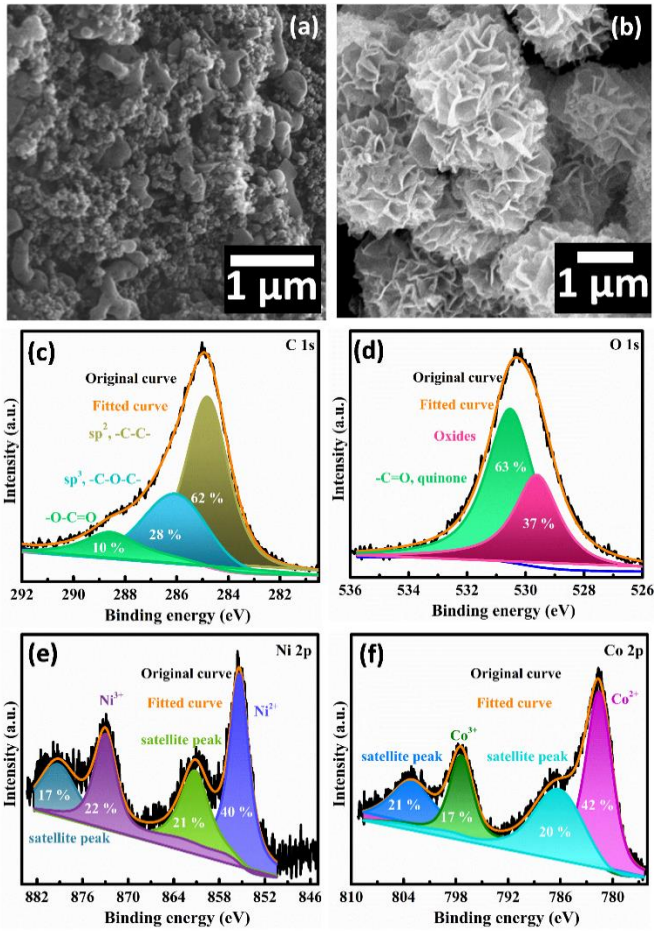

Fig. 1 SEM micrograph of (a) AC, (b) Ni-Co oxide@C-dots, XPS deconvolution spectra of Ni-Co oxide@C-dots (c) C1s, (d) O 1s, (e) Ni 2p, and (g) Co 2p

Fig. 2c illustrates the GCD profile of the device at different current densities. Here, the distortion in the curve represents the presence of pseudocapacitance. The specific capacitance of the device at different current densities is presented in Fig. 2d. The device delivers a specific capacitance of 295 F g^{-1} at a current density of 1 A g^{-1} with an excellent rate capability of 55% until 5 A g^{-1}. Fig. 2e elucidates the Coulombic efficiency iR drop of the device at different current densities. The device delivers ~65% of the coulombic efficiency at 1 A g^{-1} that reaches 100% till 20 A g^{-1}. It indicates that some electrolyte ions penetrate deep inside the pore during charging at low current density. Upon discharge, these ions get trapped, thereby decreasing the Coulombic efficiency. However, large surface area adsorption and ions desorption at high current density quickly improve the Coulombic efficiency. Also, the device shows minimal iR drop indicating high conductivity. The low resistance is due to the presence of a C-dots pocket throughout the

Ni-Co oxide that improves the conductivity of the nanocomposites. Further, Fig. 2f shows the Ragone plot of the device. Encouragingly, the device delivers a specific energy density of 92 Wh kg^{-1} at a power density of 1000 W $kg^{-1,}$ which retains till 19 Wh kg^{-1} at 20 kW kg^{1}. The inset of Fig. 2f shows a digital micrograph of the illumination of LED by an assembled asymmetric device.

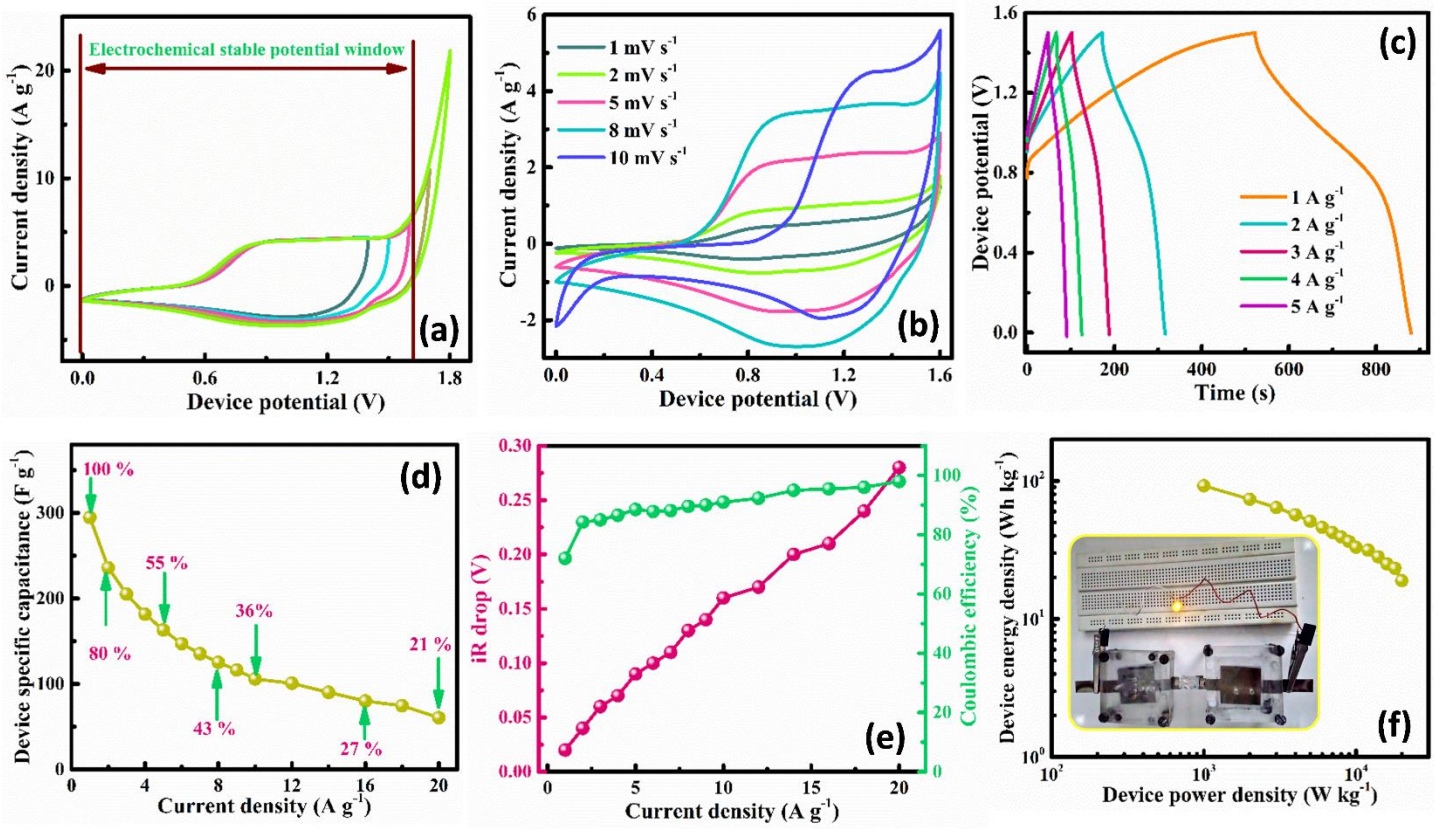

Fig. 2 Electrochemical asymmetric device Ni-Co oxide@C-dots//AC in 6 M KOH electrolyte. (a) CV curve at different potential windows at a scan rate of 50 mV s^{-1}, (b)CV curve at different scan rates, (c) GCD plot at various current densities, (d) specific capacitance, (e) Coulombic efficiency and iR drop at different current densities, and (f) Ragone plot inset: illuminated of LED by as-assembled asymmetric device

Table 1: Electrochemical parameters of asymmetric dvice Ni-Co oxide@C-dots//AC over various current densities

Current density (A g^{-1})	Specific capacitance (F g^{-1})	Coulombic efficiency (%)	iR drop (V)	Specific energy density (Wh kg^{-1})	Specific power density (W kg^{-1})
1	294.8	72.0	0.02	92.0	1000
2	236.0	84.0	0.04	73.7	2000
3	205.0	85.0	0.06	64.0	3000
4	182.0	86.0	0.07	56.8	4000
5	163.0	88.5	0.09	51.0	5000
6	147.0	87.8	0.1	46.0	6000
7	135.0	88.0	0.11	42.3	7000
8	125.0	89.6	0.13	39.0	8000
9	116.0	90.0	0.14	36.3	9000
10	106.0	91.0	0.16	33.0	10000
12	101.0	92.0	0.17	31.4	12000
14	90.0	95.0	0.2	28.1	14000
16	80.0	95.5	0.21	25.0	16000
18	74.5	96.0	0.24	23.2	18000
20	60.6	98.0	0.28	18.9	20000

5. CONCLUSIONS

The present study illustrates a low-cost and environment-friendly electrode material for supercapacitor application. The human hair was used as a precursor for the synthesis of activated carbon. For Ni-Co oxide@C-dots nanocomposites, a simple hydrothermal synthesis was employed. The SEM micrograph successfully syntheses a homogeneous nanocomposite with flower-like morphology. The XPS analysis depicts the presence of C, O, Ni, and Co functionalities. The asymmetric device assembly shows a wide operating potential window of 1.6 V. The electrochemical studies illustrate that the charges are stored by capacitive and Faradaic mechanisms providing excellent device-specific capacitance of 295 F g^{-1} with minimal resistance. The device shows a high energy density of 92 Wh kg^{-1} at a power density of 1000 W kg^{-1}. The study provides a facile approach to the synthesis and assembly of high-performance asymmetric supercapacitors.

ACKNOWLEDGEMENTS

The financial support provided by the Science and Engineering Research Board, Department of Science and Technology, India (SR/WOS-A/ ET-48/2018) for carrying out this research work is acknowledged.

REFERENCES

[1] W. Raza *et al.*, "Recent advancements in supercapacitor technology," *Nano Energy*, vol. 52, pp. 441–473, Oct. 2018, doi: 10.1016/j.nanoen.2018.08.013.

[2] B. De, T. Kuila, N. H. Kim, and J. H. Lee, "Carbon dot stabilized copper sulphide nanoparticles decorated graphene oxide hydrogel for high performance asymmetric supercapacitor," *Carbon* , vol. 122, pp. 247–257, Oct. 2017, doi: 10.1016/j.carbon.2017.06.076.

[3] P. Sinha *et al.*, "Keratin-derived functional carbon with superior charge storage and transport for high-performance supercapacitors," *Carbon* , vol. 168, pp. 419–438, Oct. 2020, doi: 10.1016/j.carbon.2020.07.007.

[4] J. Zhang, F. Liu, J. P. Cheng, and X. B. Zhang, "Binary Nickel-Cobalt Oxides Electrode Materials for High-Performance Supercapacitors: Influence of its Composition and Porous Nature," *ACS Appl. Mater. Interfaces*, vol. 7, no. 32, pp. 17630–17640, 2015, doi: 10.1021/acsami.5b04463.

[5] S. Zhang and N. Pan, "Supercapacitors Performance Evaluation," *Adv. Energy Mater.*, vol. 5, no. 6, p. 1401401, Mar. 2015, doi: 10.1002/aenm.201401401.

[6] Y. Shao *et al.*, "Design and Mechanisms of Asymmetric Supercapacitors," *Chem. Rev.*, vol. 118, no. 18, pp. 9233–9280, Sep. 2018, doi: 10.1021/acs.chemrev.8b00252.